Birefringence and optical activity of the incommensurate phase of $[N(CH_3)_4]_2ZnCl_4$

J. Kobayashi

Kagami Memorial Laboratory for Material Science and Technology, Waseda University,
2-8-26 Nishi-Waseda, Shinjuku-ku, Tokyo 169, Japan
and Research Development Corporation of Japan, 2-5-2 Nagata-cho, Chiyoda-ku, Tokyo 100, Japan

K. Saito, N. Takahashi, and I. Kamiya

Kagami Memorial Laboratory for Material Science and Technology, Waseda University,
2-8-26 Nishi-Waseda, Shinjuku-ku, Tokyo 169, Japan

By using a high-accuracy universal polarimeter, all the components of the optical-activity tensor g and birefringence Δn of $[N(CH_3)_4]_2ZnCl_4$ were measured in its paraelectric, incommensurate, and ferroelectric phases. Only one component, g_{23}, was found to appear both in the incommensurate and ferroelectric phases, but all the other components vanished in the three phases. This fact mostly disagrees with the recent report of Dijkstra, Kremers, and Meekes, but partly agrees with our previous result. It was confirmed that the paraelectric phase was optically inactive although Dijkstra, Kremers, and Meekes reported that most components of the gyration tensor were nonzero. The results for Δn agree with those of Dijkstra, Kremers, and Meekes except for Δn_a. The source of these experimental disagreements are discussed.

I. INTRODUCTION

In most of the A_2BX_4 family crystals, incommensurate (abbreviated IC) phases appear before their paraelectric phases transform into ferroelectric or ferroelastic phases. It was long believed that the structure of an IC phase should be centrosymmetrical. Kobayashi and Uesu[1] developed a general method designated HAUP (high-accuracy universal polarimeter) for simultaneously measuring the optical activity, birefringence, and rotation of the indicatrix of any solids. Kobayashi et al.[2] applied it to an IC phase of $(NH_4)_2BeF_4$, and discovered optical activity (OA) in the IC phase. Subsequently, they[3-5] found OA in the IC phases of a few crystals of the same family. One of the salient features of the HAUP method was to remove exhaustively systematic errors, which had been overlooked for ordinary polarimetric measurements, but should be critical for measurements of OA. It was significant that Kobayashi, Kumomi, and Saito[6] found a systematic error called $\delta\Upsilon$, three years after the invention of HAUP, which took place in setting up a crossed Nicols system. They developed a method for removing it in the refined HAUP method. Meekes and Janner[7] were successful in finding a nonzero gyration-tensor component g_{23} in the IC phase of Rb_2ZnBr_4 by using the refined HAUP method. They also showed that some Fourier components of the gyration tensor were permitted by the centrosymmetrical superspace-group symmetry, and derived a selection rule for the appearance of gyration-tensor components of an IC phase. On the other hand, Kobayashi[8] interpreted this as an essential origin of OA of an IC phase. He ascribed it to the existence of a dynamical helical wave (phason) in the IC phase as the result of condensation of a complex phonon mode. According to this theory, the IC phases should be weakly axially symmetrical, and therefore permit OA. Kobayashi and co-workers further reported the occurrence of OA in the IC phases of $[N(CH_3)_4]_2ZnCl_4$ (ab-breviated TMAZC),[9] $[N(CH_3)_4]_2CuCl_4$,[10] and Rb_2ZnCl_4.[11] However, these data were confined to only one component among six of the gyration tensor in each IC phase.

Recently, Dijkstra, Kremers, and Meekes[12] performed comprehensive HAUP measurements of OA and birefringence of TMAZC using six specimens with different orientations. They found that all the components g_{ij}—except for g_{11}—existed not only in the IC phase, but also in the paraelectric phase. However, they described that the measured OA was different from sample to sample. This fact made it difficult for us to conceive of their data as decisive. They used essentially the same method as that of Moxon and Renshaw[13] for evaluating the systematic errors of HAUP. Moreover, they stressed that the derivation of a gyration-tensor component of TMAZC by Kobayashi et al.[6] was based on an assumption that the paraelectric phase of TMAZC was optically inactive. They also criticized the birefringence result of the authors.[14] We considered it necessary to make a detailed study of all the components of the gyration tensor and birefringence of TMAZC in order to elucidate the optical properties of TMAZC. This paper reports the results of the study.

II. HAUP EXPERIMENTS

A. Specimens

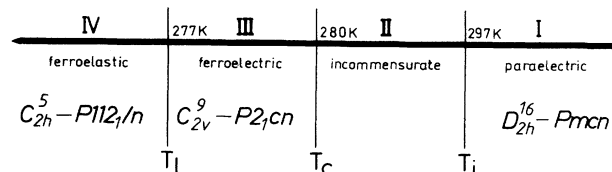The phase diagram of TMAZC in the relevant temperature region is shown schematically in Fig. 1, the transi-

FIG. 1. Schematic representation of the phase diagram of $[N(CH_3)_4]_2ZnCl_4$.

tion temperatures separating the phases I, II, III, and IV being defined T_i, T_c, and T_l, as indicated in the figure. Phase I in the paraelectric state is centrosymmetrical, the space group[15] being orthorhombic D_{2h}^{16} with lattice constants $a = 8.998$ Å, $b = 15.541$ Å, and $c = 12.276$ Å. An IC modulation of the superlattice in phase II takes place along the c axis, and the commensurate superlattice is recovered in phase III with a period of $5c$. The spontaneous polarization P_s appears along the a axis in phase III. The principal axes x_1, x_2, and x_3 of the dielectric impermeability tensor are taken along the crystallographic a, b, and c axes of phase I in what follows. Notice that Dijkstra et al.[12] took x_1 and x_2 axes along the crystallographic b and a axes, the reverse of our system.

The crystals were grown by cooling an aqueous solution of $N(CH_3)_4Cl$ and $ZnCl_2$ in 2:1 molar ratio from 308.0 to 302.5 K with a cooling rate of -0.24 K/d. The crystals obtained were colorless.

As the first step of the present study, the optical nature of TMAZC was determined by using a quartz wedge equipped with a polarizing microscope. An optical orientation of phase I at 315 K is expressed in Fig. 2(a) by a stereographic projection along the a axis; a, b, and c axis were found to be X, Z, and Y axes optically, and, accordingly, the (001) plane was the optic plane. This fact was confirmed by a conoscopic figure of the same orientation of the specimen, as shown in Fig. 2(b). Although clear melatopes were not seen owing to a small value of Δn_a, the optic plane was definitely discerned. When temperature of the specimen was cooled to 309 K, the crystal became isotropic along the a axis, and, by further cooling, the optic plane was changed to the (010) plane, as shown in Fig. 2(c).

We prepared six specimens with surface planes of the following indices: (100), (010), (001), (110), (101), and (011). Finally, each specimen was polished using alumina powder with a homogeneous grain size of 0.2 μm.

When light was incident perpendicular to (100), (010), and (001) specimens, the following birefringence and gyration could be measured: $\Delta n_{(100)} \equiv \Delta n_a = n_c - n_b$, $\Delta n_{(010)} \equiv \Delta n_b = n_c - n_a$, $\Delta n_{(001)} \equiv \Delta n_c = n_b - n_a$, and $G_{(100)} = g_{11}$, $G_{(010)} = g_{22}$, and $G_{(001)} = g_{33}$.

$\Delta n_{(110)}$, which could be measured by using the (110) specimen, can be expressed in terms of Δn_a and Δn_b in the following way. Let the wave vector of the incident light be designated by $s(s_1, s_2, s_3)$ with $s_1 = \cos\theta$,

$s_2 = \sin\theta$, and $s_3 = 0$, where θ is an angle made by s and the x_1 axis in the (001) plane. Then B, the dielectric impermeability normal to the s direction, is expressed as

$$B = \frac{1}{n^2} = B_{11}\sin^2\theta + B_{22}\cos^2\theta , \qquad (1)$$

where B_{11} and B_{22} are eigenvalues of the B tensor, and related to the refractive indices n_a and n_b by $B_{11} = 1/n_a^2$ and $B_{22} = 1/n_b^2$. Then,

$$n = \frac{n_a n_b}{\sqrt{n_a^2\cos^2\theta + n_b^2\sin^2\theta}} . \qquad (2)$$

By substituting $n_a = n_b - \Delta n_c$ into (2),

$$n = \frac{n_b(1 - \Delta n_c/n_b)}{\sqrt{1 - 2(\Delta n_c/n_b)\cos^2\theta + (\Delta n_c/n_b)^2\cos^2\theta}} . \qquad (3)$$

This can be expanded in terms of a small quantity, $\Delta n_c/n_b$,

$$n \simeq n_b[1 - (\Delta n_c/n_b)\sin^2\theta]$$
$$= n_a\sin^2\theta + n_b\cos^2\theta .$$

Therefore,

$$\Delta n_{(110)} = n_c - n = (n_c - n_a)\sin^2\theta + (n_c - n_b)\cos^2\theta$$
$$= \Delta n_b\sin^2\theta + \Delta n_a\cos^2\theta .$$

As $\theta \simeq 30°$, from lattice constants a and b,

$$\Delta n_{(110)} = 0.25\Delta n_b + 0.75\Delta n_a \qquad (4)$$

and

$$G_{(110)} = 0.75g_{11} + 0.25g_{22} + 0.86g_{12} . \qquad (5)$$

The same treatments could be applied to the (101) and (011) specimens. The number, index of the surface perpendicular to the light beam, birefringence and gyration to be measured, area, and thickness of each specimen are tabulated in Table I. Dijkstra et al.[12] also used six specimens; among them, four specimens were the same as our specimen nos. 1–3 and 6, but others corresponded to our nos. 4 and 5, with $\theta = 45°$ for each case.
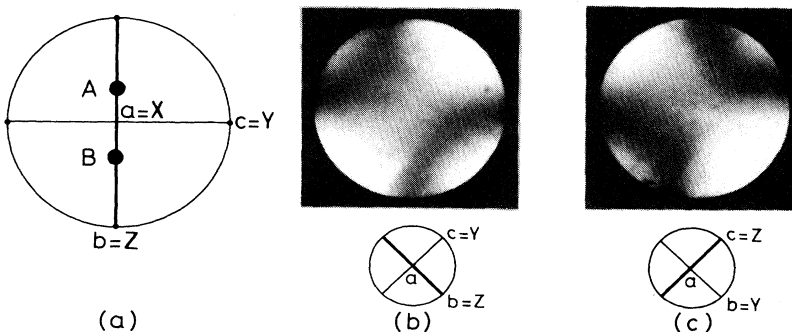

(a)   (b)   (c)

FIG. 2. Optical nature of $[N(CH_3)_4]_2ZnCl_4$. (a) Stereographic projection of the optical orientation at 315 K, (b) conoscopic figure at 313 K, and (c) conoscopic figure at 297 K.

J. KOBAYASHI, K. SAITO, N. TAKAHASHI, AND I. KAMIYA

TABLE I. Data for specimens used in the present experiment.

Sample no.	Surface planes	Birefringence Δn	Gyration G	Area (mm^2)	Thickness (mm)
1	(100)	$\Delta n_a = n_c - n_b$	$G_a = g_{11}$	2.3×3.3	5.126
2	(010)	$\Delta n_b = n_c - n_a$	$G_b = g_{22}$	1.8×2.8	1.300
3	(001)	$\Delta n_c = n_b - n_a$	$G_c = g_{33}$	1.7×3.4	1.330
4	(110)	$\Delta n_{(110)} = 0.75 \Delta n_a + 0.25 \Delta n_b$	$G_{(110)} = 0.75 g_{11} + 0.25 g_{22} + 0.86 g_{12}$	1.8×3.2	1.995
5	(101)	$\Delta n_{(101)} = 0.34 \Delta n_c - 0.66 \Delta n_a$	$G_{(101)} = 0.66 g_{11} + 0.34 g_{33} + 0.95 g_{13}$	2.2×4.2	2.085
6	(011)	$\Delta n_{(011)} = 0.62 \Delta n_c + 0.38 \Delta n_b$	$G_{(011)} = 0.38 g_{22} + 0.62 g_{33} + 0.97 g_{23}$	2.0×3.3	1.350

B. Measurements

HAUP measurements were carried out on the specimens placed in a vacuum chamber and held at various temperatures within an accuracy of ± 0.02 K. The light source was a He-Ne laser with a wavelength of 6328 Å. At various temperatures, $B(0)$, retardations Δ, and characteristic angles θ_0 were measured. These quantities are written as

$$\Delta = \frac{2\pi d}{\lambda} \left[\Delta n^2 + \left[\frac{G}{\bar{n}} \right]^2 \right]^{1/2} , \quad (6a)$$

$$B(0) = (\gamma - 2k)\sin\Delta + 2\delta\Upsilon \cos^2(\Delta/2) , \quad (6b)$$

or, equivalently,

$$B(0)/\sin\Delta = \gamma - 2k + \delta\Upsilon \cot(\Delta/2) , \quad (6c)$$

and

$$\theta_0 = -\tfrac{1}{2}(p+q)\cot(\Delta/2) - \tfrac{1}{2}\delta\Upsilon + \Psi . \quad (6d)$$

Here, d represents the thickness of the specimen, k, the ellipticity of the elliptically polarized wave traveling in the specimen, Ψ the rotation angle of the indicatrix, and $\bar{n}$ the mean refractive index. $\gamma = p - q$ and $\delta\Upsilon$ are the principal systematic errors. p and q^1 represent the parasitic ellipticities of the polarizer and analyzer, respectively. The operation of setting up the crossed Nicols system without a specimen can be made with the maximum accuracy within the limit of p and q. However, when a specimen is inserted between the polarizer and analyzer, a slight refraction of the light beam by the specimen cannot be avoided, since the surface of the specimen are not oriented strictly perpendicular to the light beam. Therefore the accurate condition of the crossed Nicols system is shifted there. This error is $\delta\Upsilon^6$. If a specimen is optically inactive, i.e., $k = 0$, (6c) indicates that $B(0)/\sin\Delta$ changes linearly with respect to $\cot(\Delta/2)$. The same is the case for θ_0, when $\Psi = 0$, from (6d). From the relations of (6c) and (6d), γ (or p and q) and $\delta\Upsilon$ can be obtained straightforwardly when $\Psi = k = 0$. Even when k is strongly dependent on temperature, $\delta\Upsilon$ can be acquired from a $B(0)$-versus-temperature curve. The value of $B(0)$, at a temperature where $\Delta = 2n\pi$ (n are integers) equals $2\delta\Upsilon$, this tempera-

ture being determined directly from a Δ-versus-temperature curve, or indirectly by the divergence of θ_0.

When $k \neq 0$, the evaluation of k and γ (or p and q) can be made by the following four methods.

Method (1):[6] When a specimen contains an optically inactive phase, e.g., centrosymmetrical phase, γ can be determined there by setting $k = 0$ in (6c). This γ value can be used for deriving k in the optically active phases.

Method (2):[16] p can be determined by using an optically inactive standard crystal, e.g., $LiNbO_3$. It is defined as $\hat{p}$, in order to emphasize that it is related to both the optical system of the standard crystal and that of the specimen. Further, $\hat{p} + q$ of the specimen system can be determined by (6d). Thus, $\gamma = \hat{p} - q$ can be calculated.

Method (3):[1] Exchange of order of polarizer and analyzer results in a reversal of the sign of γ. Then we can obtain γ and k separately. However, γ and $\delta\Upsilon$ cannot be kept constant when the two elements are exchanged. Therefore this method cannot be practicable.

Method (4):[13] The rotation of a specimen by 90° causes a change of sign in both the phase and ellipticity, i.e., $\Delta \rightarrow -\Delta$ and $k \rightarrow -k$. This operation also enables one to calculate γ and k separately. However, it must be noted that q (and, accordingly, γ) and $\delta\Upsilon$ should be changed by the rotation. Moxon et al.[13] ignored the former and ascribed the latter to mechanical inaccuracies of the motor drive. From the nature of $\delta\Upsilon$ it seems unlikely that their interpretation was perfectly correct.

HAUP measurements were performed at first on the (011) (no. 6) specimen in the temperature range from 319 K down to 278 K, with due attention to the fact that Dijkstra et al.[12] found OA along this direction not only in the IC phases, but in the paraelectric phases. As a measure of the quality of the present optical system, the extinction ratio, i.e., ratio of the intensity of the emergent light from the crossed Nicols system with respect to that of the incident light, reached 6×10^{-9}. This condition enabled us to determine the extinction positions of the specimen very accurately by rotating the crossed Nicols system at 11 intervals within the total range of about $\pm 4 \times 10^{-3}$ deg.

The temperature dependences of $B(0)$, $\Delta/2$, and θ_0 of specimen no. 6 are shown in Figs. 3(a), 3(b), and 3(c), respectively. The dependence of Δ broke abruptly at T_i, but not at T_c. That of θ_0 manifested a divergent behavior at 288 K, where $\Delta = 0$. At this temperature $\delta\Upsilon$ could be evaluated as -3.90×10^{-4} from Fig. 3(a). The depen-

dences of $B(0)/\sin\Delta$ and θ_0 on $\cot(\Delta/2)$ are shown in Figs. 4(a) and 4(b). As can be seen in the inset of Fig. 4(a), $B(0)/\sin\Delta$ changed linearly with respect to $\cot(\Delta/2)$ for a narrow range of Δ values of the paraelectric phase. This meant that k and γ were kept constant in the paraelectric phase. In order to separate both constants, method (2) was applied by using $LiNbO_3$: (100)-plane specimen with an area of 3.1×4.3 mm^2 and a thickness of 0.234 mm. Figures 5(a) and 5(b) depict the linear relationships of $B(0)/\sin\Delta$ and θ_0 of this crystal with respect to $\cot(\Delta/2)$, respectively. From the former the systematic error $\gamma'=\hat{p}-q'$ was determined to be 7.02×10^{-4}, while $\hat{p}+q'$ was determined to be -0.58×10^{-4} from the latter. Adding the two quantities, we determined $\hat{p}=3.22\times10^{-4}$. On the other hand,

FIG. 4. Relations of (a) $B(0)/\sin\Delta$ and (b) θ_0 with respect to $\cot(\Delta/2)$ for (011) specimen of $[N(CH_3)_4]_2ZnCl_4$. The inset in (a) depicts relation of $B(0)/\sin\Delta$ with respect to $\cot(\Delta/2)$ in the paraelectric phase.
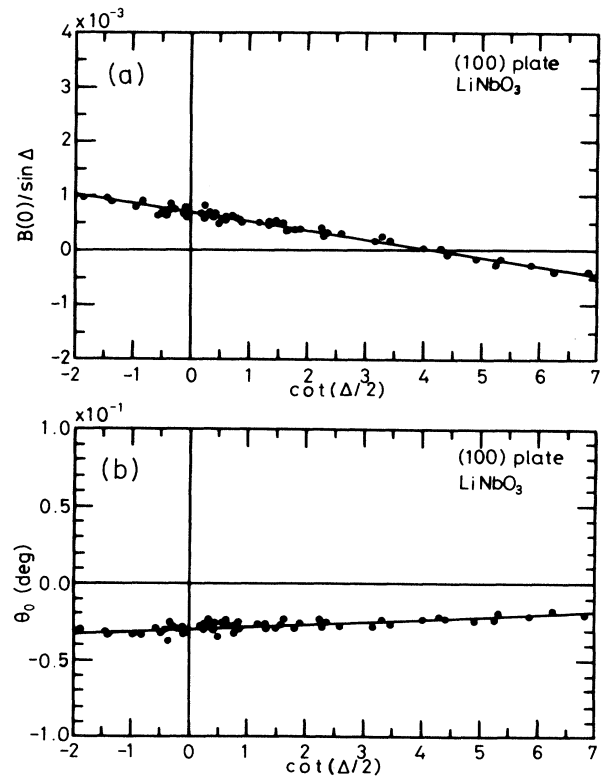

FIG. 3. Temperature dependences of (a) $B(0)$, (b) $\Delta/2$, and (c) θ_0 of (011) specimen of $[N(CH_3)_4]_2ZnCl_4$.

FIG. 5. Relations of (a) $B(0)/\sin\Delta$ and (b) θ_0 with respect to $\cot(\Delta/2)$ for (100) specimen of $LiNbO_3$.
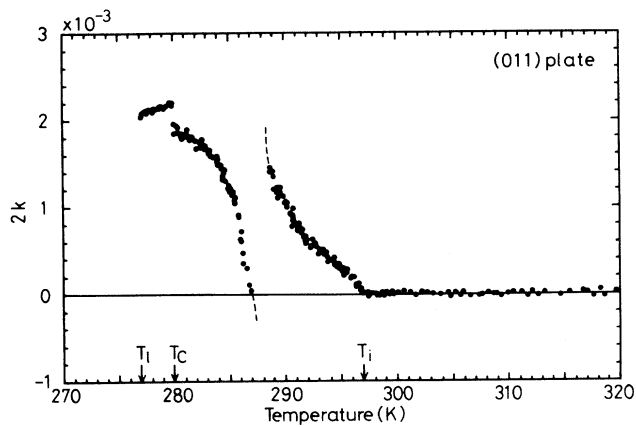
$\hat{p} + q$ of the specimen system was evaluated as -2.08×10^{-4} from Fig. 4(b). Thus we could obtain $\gamma = \hat{p} - q = 8.52 \times 10^{-4}$. By using γ and $\delta\Upsilon$, $2k$ was calculated as shown in Fig. 6. From the figure it is clear that k was kept zero in the paraelectric phase. Then, the temperature dependences of $G_{(011)}$ and $\Delta n_{(011)}$ were acquired as depicted in Fig. 7, and it is seen that $G_{(011)}$ appeared at T_i, but leveled off immediately when the temperature decreased. It became zero at 287 K, increased its modulus afterwards, and jumped to larger values in phase III. $G_{(011)}$ is undoubtedly kept zero in the paraelectric phase. The $G_{(011)}$ measured by Dijkstra et al.[12] are indicated by a dashed line for the sake of comparison. They partly resemble our data in the IC
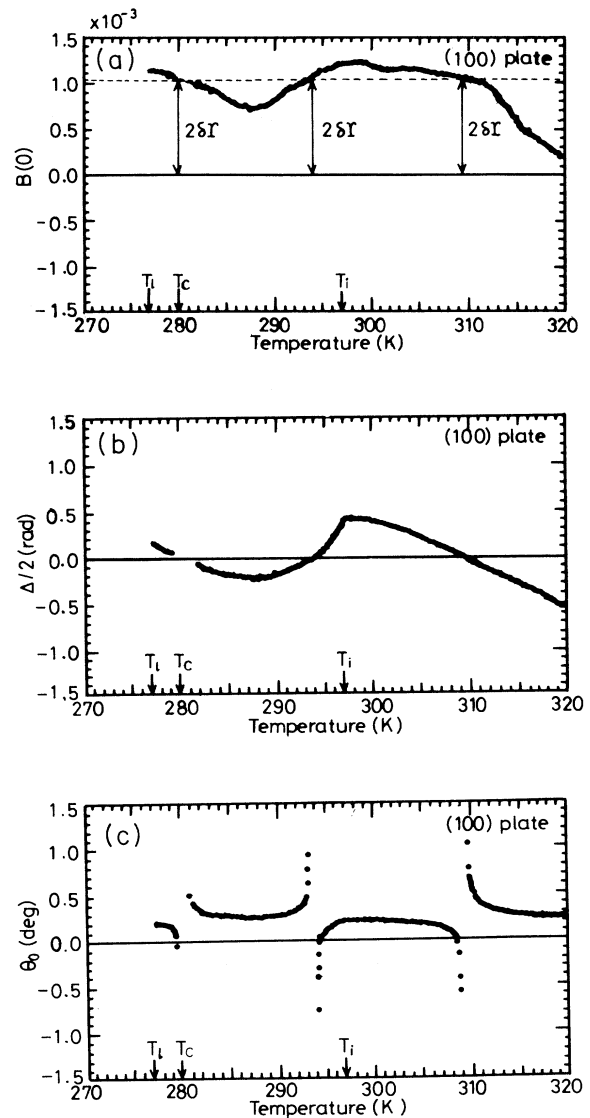
FIG. 6. Temperature dependence of $2k$ for (011) specimen of $[N(CH_3)_4]_2ZnCl_4$.
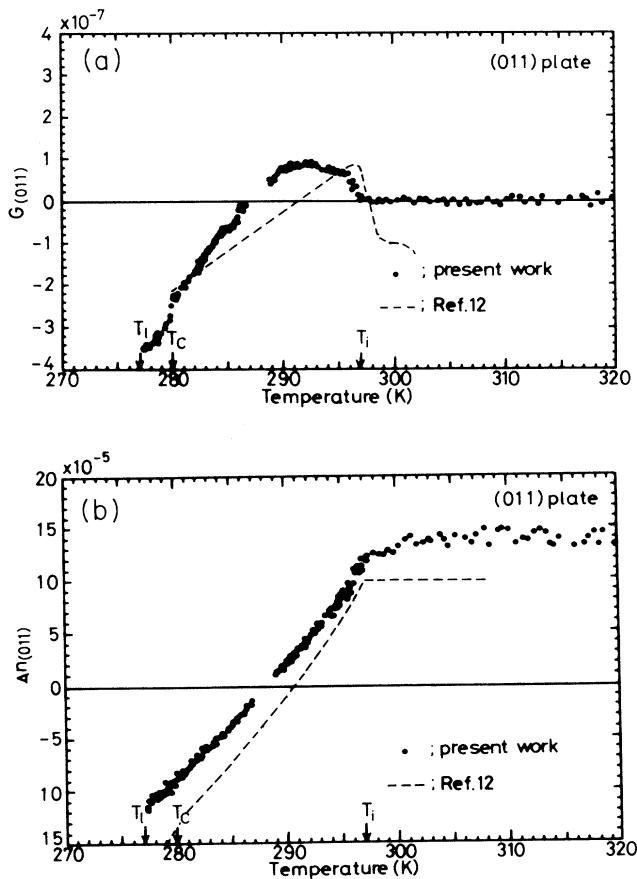
FIG. 7. Temperature dependences of (a) $G_{(011)}$ and (b) $\Delta n_{(011)}$ of $[N(CH_3)_4]_2ZnCl_4$.

FIG. 8. Temperature dependences of (a) $B(0)$, (b) $\Delta/2$, and (c) θ_0 of (100) specimen of $[N(CH_3)_4]_2ZnCl_4$.
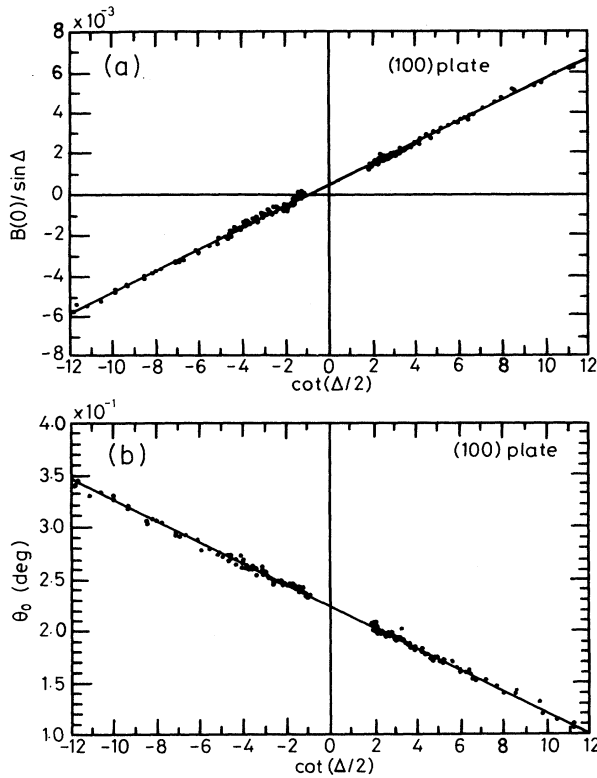
FIG. 9. Relations of (a) $B(0)/\sin\Delta$ and (b) θ_0 with respect to $\cot(\Delta/2)$ for (100) specimen of $[N(CH_3)_4]_2ZnCl_4$.
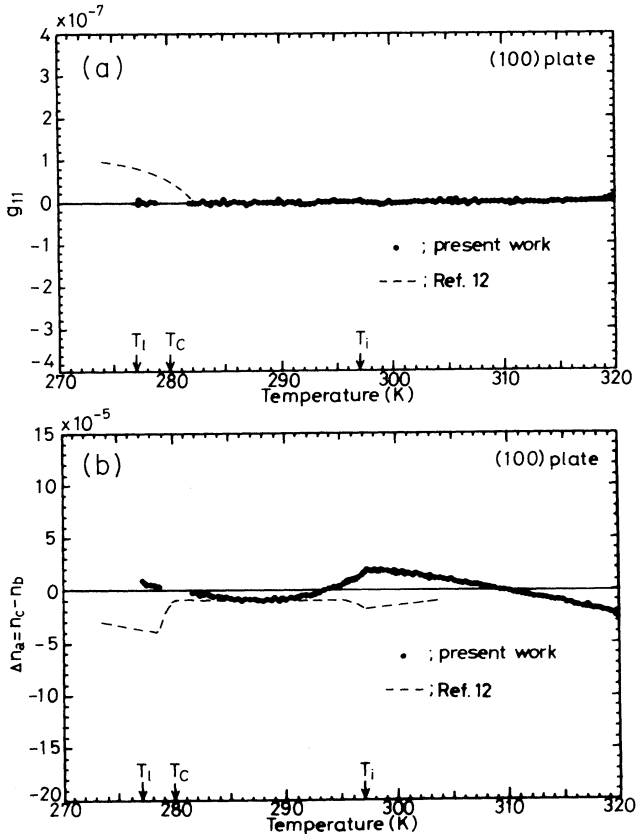

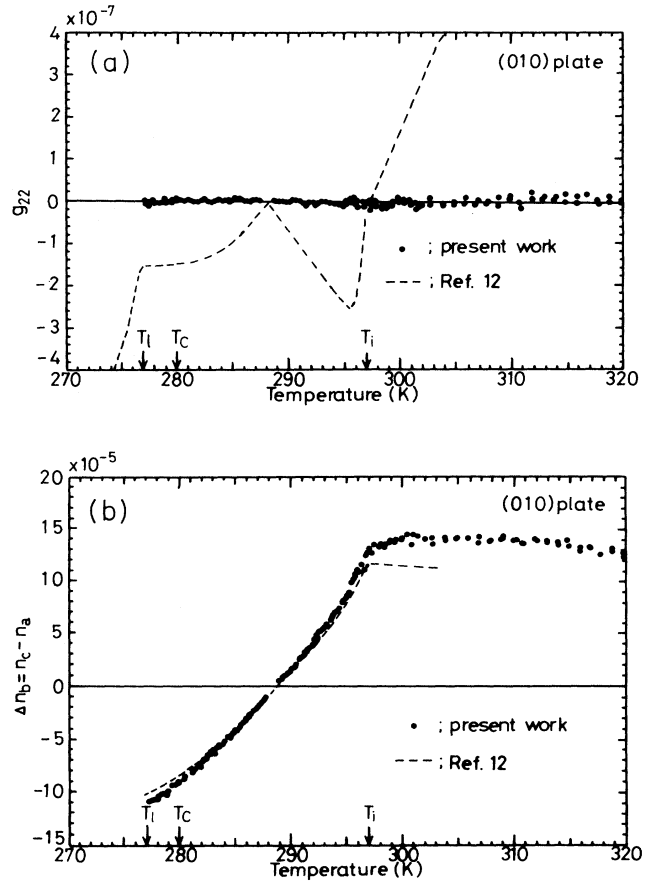FIG. 10. Temperature dependences of (a) g_{11} and (b) Δn_a of $[N(CH_3)_4]_2ZnCl_4$.

FIG. 11. Temperature dependences of (a) g_{22} and (b) Δn_b of $[N(CH_3)_4]_2ZnCl_4$.

phase, but are not zero in the paraelectric phase. This fact conflicts with our results. The temperature dependences of $\Delta n_{(011)}$ measured by the two groups approximately agree.

Next, measurements were performed on the (100) (no. 1) specimen. The temperature dependences of $B(0)$, $\Delta/2$, and θ_0 are depicted in Figs. 8(a), 8(b), and 8(c), respectively. The dependence of θ_0 manifested typical divergent behavior at 309, 294, and 280 K, where Δ became zero. $B(0)/\sin\Delta$ and θ_0 are plotted with respect to

TABLE II. Systematic errors in the six optical systems

Sample no.	p ($\times 10^{-4}$)	q ($\times 10^{-4}$)	γ ($\times 10^{-4}$)	$\delta\Upsilon$ ($\times 10^{-4}$)
1	3.98	−0.32	4.30	5.04
2	2.40	−2.18	4.58	−7.37
3	1.93	7.97	−6.04	8.61
4	−0.59	3.75	−4.34	4.38
5	−3.52	7.58	−11.10	−3.81
6	3.22	−5.30	8.52	−3.90

cot($\Delta/2$) in Figs. 9(a) and 9(b), respectively. It is clearly seen that $B(0)/\sin\Delta$ changed strictly in a linear way, indicating that k was kept constant irrespective of the change of temperature. Here we again applied method (2) to deduce whether k was zero or not. As a result, we clearly knew that $k=0$, but the description of the process is omitted. γ and $\delta\Upsilon$ were obtained as 4.30×10^{-4} and 5.04×10^{-4}, respectively. The linear variation of θ_0 showed invariance of ψ. This invariance of ψ, which was already found in Fig. 4(b) for specimen no. 6 and will be observed in the rest of the specimens, indicates that the indicatrix of TMAZC does not rotate with the change of temperature in its paraelectric, IC, and ferroelectric phases. This fact also implies the validity of the symmetries of the two phases indicated in Fig. 1. We could calculate g_{11} and Δn_a as a function of temperature as depicted in Figs. 10(a) and 10(b), respectively. In both figures the results of Dijkstra et al.[12] were also indicated by dashed lines. g_{11} is clearly zero in the measured temperature range. The results of both groups agree, except in phase III. Δn_a becomes zero and changes its sign at 309, 294, and 280 K, while Dijkstra et al.[12] did not find

this phenomenon. Vlokh et al.[17] already found that Δn_a became zero at nearly 292 K.

Similar measurements were performed on specimen nos. 2–5. The strictly linear relations of $B(0)/\sin\Delta$ and θ_0 were composed to cot($\Delta/2$) for these specimens. The systematic errors observed in every specimen are tabulated in Table II, where p and q values are scattered since different optical systems were used for each specimen. The temperature dependences of the gyration and birefringence of specimen nos. 2–5 are represented in Figs. 11–14. In all the orientations of TMAZC indicated in these figures, gyration did not take place at all in the mentioned temperature range. It follows that g_{22}, g_{33}, g_{12}, and g_{13} are zero in the paraelectric, IC, and ferroelectric phases. This fact also indicates that $G_{(011)}$ nearly equals g_{23}. In contrast to our observations, Dijkstra et al.[12] reported that these components appeared in the IC and paraelectric states, as depicted by dashed lines partly in Figs. 11 and 12. Thus, distinct differences were clarified between the results of these components measured by both groups. The Δn_b and Δn_c measured by both groups nearly coincided.
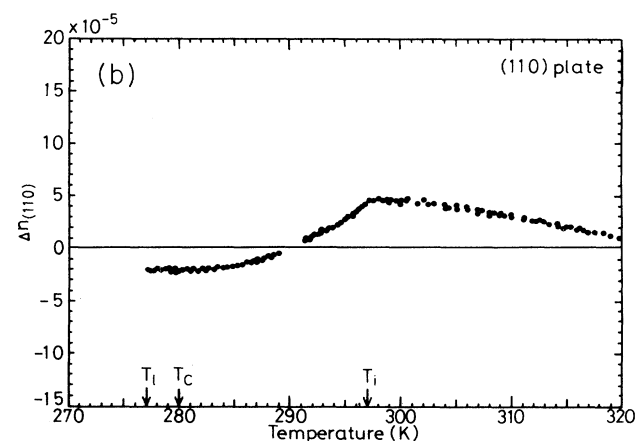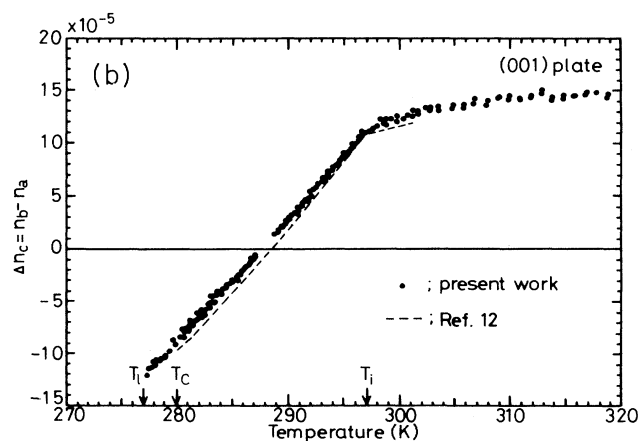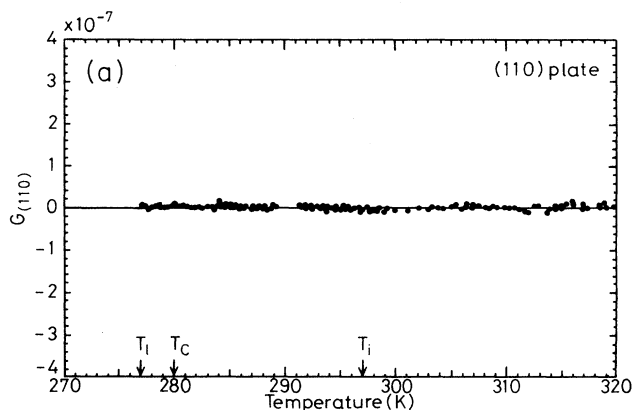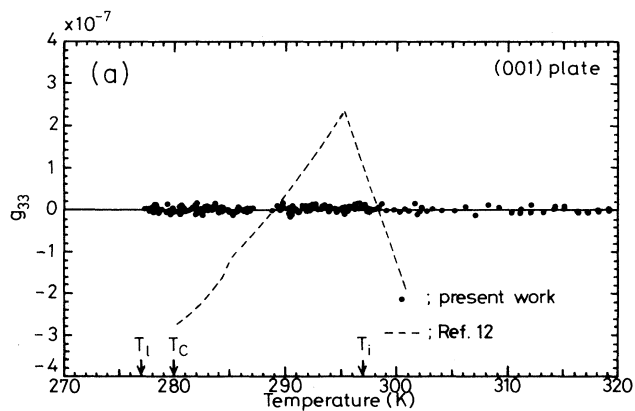

FIG. 12. Temperature dependences of (a) g_{33} and (b) Δn_c of [N(CH$_3$)$_4$]$_2$ZnCl$_4$.

FIG. 13. Temperature dependences of (a) $G_{(110)}$ and (b) $\Delta n_{(110)}$ of [N(CH$_3$)$_4$]$_2$ZnCl$_4$.
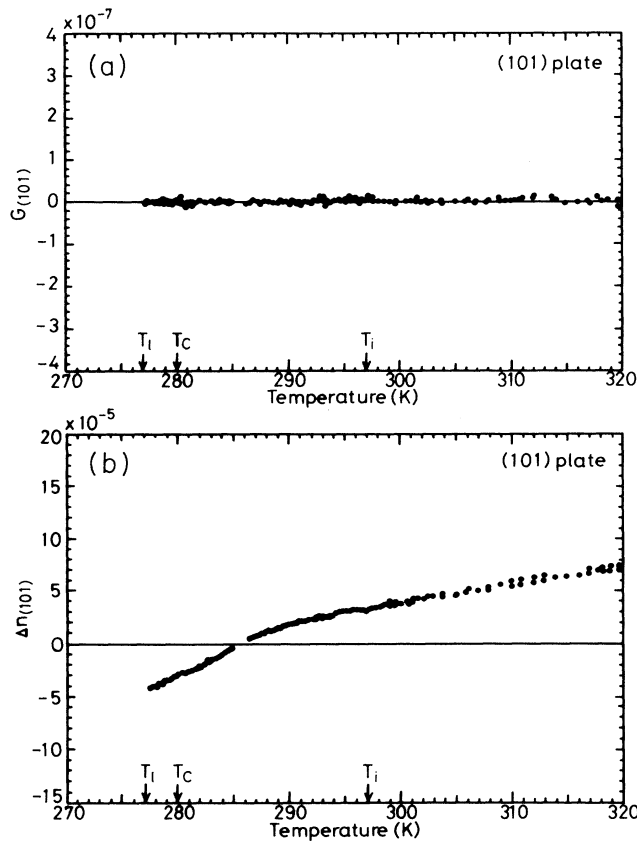
FIG. 14. Temperature dependences of (a) $G_{(101)}$ and (b) $\Delta n_{(101)}$ of $[N(CH_3)_4]_2ZnCl_4$.

FIG. 15. Temperature dependence of g_{23} of $[N(CH_3)_4]_2ZnCl_4$.

FIG. 16. Temperature dependences of Δn_a, Δn_b, and Δn_c of $[N(CH_3)_4]_2ZnCl_4$.

FIG. 17. Temperature dependences of $\Delta n_{(110)}$, $\Delta n_{(101)}$, and $\Delta n_{(011)}$ of $[N(CH_3)_4]_2ZnCl_4$.

III. DISCUSSION

We found that among six components of the gyration tensor only g_{23} appears in the IC and ferroelectric phases of TMAZC. Dijkstra et al.[12] insisted that only g_{11} is zero, but all the others exist in both paraelectric and IC phases, although their temperature dependences seem strange. They failed to obtain the exact values of the off-diagonal components of the gyration tensor because OA in their measurements was sample dependent, and it was not possible to measure more than one direction in one sample.

We determined the systematic errors γ and $\delta\Upsilon$ by using our own two methods[6,16] complimentarily. However, Dijkstra et al.[12] used method (4) proposed by Moxon and Renshaw.[13] It is important to note that γ and $\delta\Upsilon$ should be changed at the different extinction directions (defined here as A and B) in this method, as has already mentioned. In reality, Dijkstra, Meekes, and Kremers[18] themselves realized that the difference between $\delta\Upsilon^4$ and $\delta\Upsilon^8$ would occur, but were not successful in evaluating $\delta\Upsilon^A$, $\delta\Upsilon^B$, and k accurately. Besides, they did not pay attention to the change of γ that would occur upon the change of extinction positions of the specimen. In our present study there were not any assumptions made for deducing systematic errors. It is very likely that conspi-
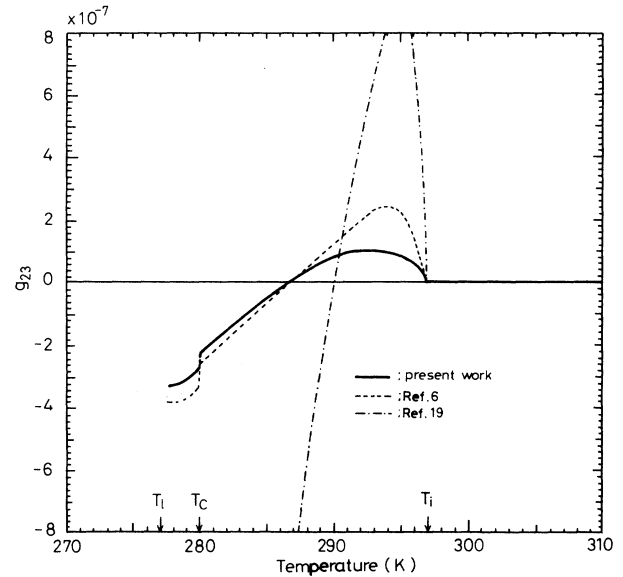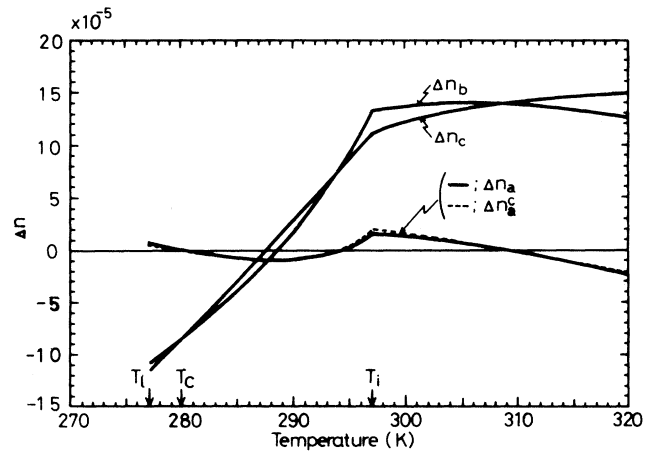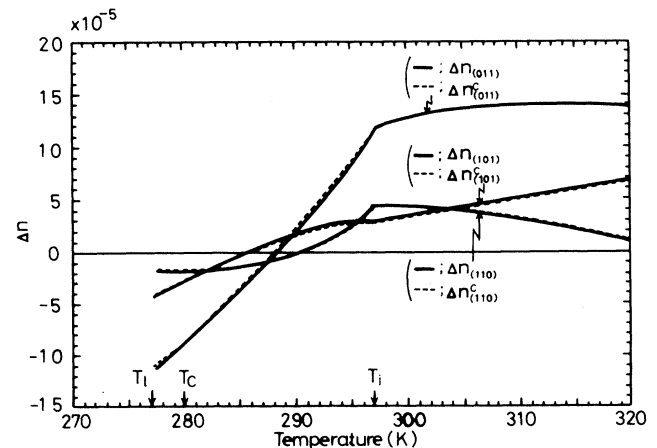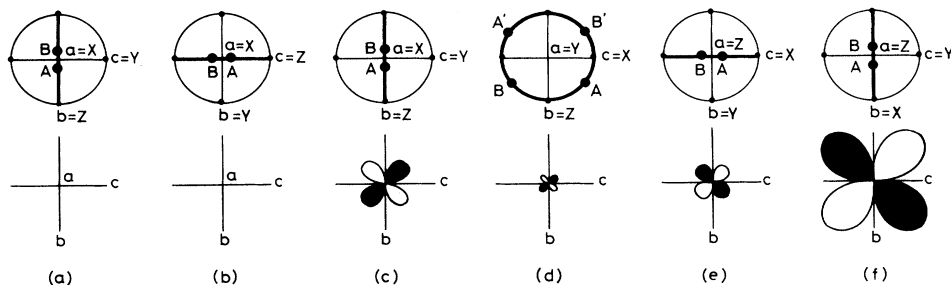
FIG. 18. Optical orientations and gyration surfaces of $[N(CH_3)_4]_2ZnCl_4$ at (a) 313 K, (b) 297 K, (c) 292 K, (d) 288 K, (e) 283 K, and (f) 278 K.

cuous differences in the results of both groups originate in these different procedures for correcting the systematic errors.

Our previous temperature-dependence data[6] for g_{23} are compared with the present results in Fig. 15, where the data of Dijkstra and Janner[19] are also depicted for comparison. The maximum value of g_{23} in the present case is about half of the previous one, although the other parts of the temperature dependence are almost the same. This difference should be, of course, brought about by improvement in the accuracy of the present measurements. The maximum value of Dijkstra and Janner[19] is 1 order of magnitude larger than ours, and the inversion temperature of the sign of g_{23} is also different.

The temperature changes of Δn_a, Δn_b, and Δn_c are summarized in Fig. 16. Their signs are altered at different temperatures. Nevertheless, the calculated values of $\Delta n_a^c = \Delta n_b - \Delta n_c$, depicted by a dashed line in the figure, completely coincided with that of Δn_a. More-

over, the calculated values of $\Delta n_{(110)}^c$, $\Delta n_{(101)}^c$, and $\Delta n_{(011)}^c$ are compared with the observed ones in Fig. 17. The agreement is excellent. In Fig. 18, changes in the gyration surfaces and optical orientations of TMAZC are illustrated.

Finally, we would like to comment on the reason for the disagreement in Δn_a. Dijkstra et al.[12] insisted that $\Delta n_a = n_b - n_c$ was always positive. This was not correct according to our observation of the optical nature of TMAZC. Besides, if Δn_a, were to be taken as $n_c - n_b$, as in our case, then the values of Δn_a^c calculated from their values of Δn_b and Δn_c will resemble our Δn_a in terms of changing sign three times in the relevant temperature range.

ACKNOWLEDGMENTS

[1]J. Kobayashi and Y. Uesu, J. Appl. Crystallogr. **16**, 204 (1983).

[2]J. Kobayashi, Y. Uesu, J. Ogawa, and Y. Nishihara, Phys. Rev. B **31**, 4569 (1985).

[3]J. Kobayashi, Ferroelectrics **50**, 53 (1983).

[4]Y. Uesu and J. Kobayashi, Ferroelectrics **64**, 115 (1985).

[5]K. Saito, I. Kunishima, J. Kobayashi, and Y. Uesu, Ferroelectrics **64**, 137 (1985).

[6]J. Kobayashi, H. Kumomi, and K. Saito, J. Appl. Crystallogr. **19**, 377 (1986).

[7]H. Meekes and A. Janner, Phys. Rev. B **38**, 8075 (1988).

[8]J. Kobayashi, Phys. Rev. B **42**, 8332 (1990).

[9]J. Kobayashi and K. Saito, Proc. Jpn. Acad. **62**, 177 (1986).

[10]K. Saito, H. Sugiya, and J. Kobayashi, J. Appl. Phys. **68**, 732 (1990).

[11]J. Kobayashi, K. Saito, H. Fukase, and K. Matsuda, Phase Transitions **15**, 225 (1988).

[12]E. Dijkstra, M. Kremers, and H. Meekes, J. Phys. Condens. Matter **4**, 715 (1992).

[13]J. R. L. Moxon and A. R. Renshaw, J. Phys. Condens. Matter **2**, 6807 (1990).

[14]K. Saito, T. Kawabe, and J. Kobayashi, Ferroelectrics **75**, 153 (1987).

[15]J. R. Wiesner, R. C. Srivastava, C. H. L. Kennard, M. D. Varia, and E. C. Lingafelter, Acta Crystallogr. **23**, 565 (1967).

[16]J. Kobayashi, T. Asahi, S. Takahashi, and A. M. Glazer, J. Appl. Crystallogr. **21**, 479 (1988).

[17]O. G. Vlokh, A. V. Kityk, and I. I. Polovinko, Opt. Spektrosk. **62**, 221 (1987) [Opt. Spectrosc. (USSR) **62**, 134 (1987)].

[18]E. Dijkstra, H. Meekes, and M. Kremers, J. Phys. D **24**, 1861 (1991).

[19]E. Dijkstra and A. Janner, Ferroelectrics **105**, 113 (1990).

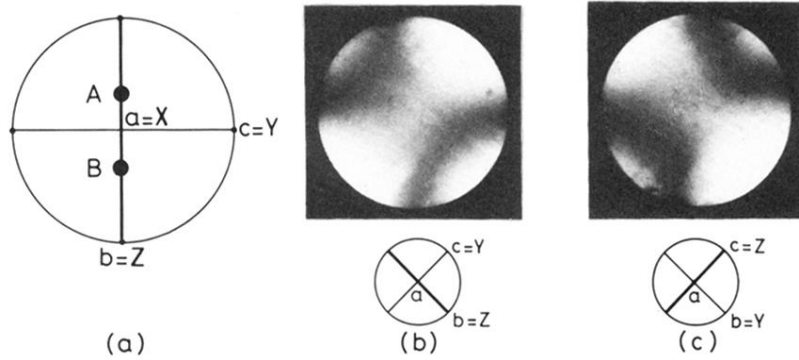FIG. 2. Optical nature of $[N(CH_3)_4]_2ZnCl_4$. (a) Stereographic projection of the optical orientation at 315 K, (b) conoscopic figure at 313 K, and (c) conoscopic figure at 297 K.